Enhancement of Reliability in Condition Monitoring Techniques in Wind Turbines

1st Rana Moeini
WMG, University of Warwick
Coventry, UK
Rana.Moeini@warwick.ac.uk

2nd Paul Weston
BCCRE, University of Birmingham
Birmingham, UK
p.weston@bham.ac.uk

3rd Pietro Tricoli
BCCRE, University of Birmingham
Birmingham, UK
P.Tricoli@bham.ac.uk

4th Truong-Quang Dinh
WMG, University of Warwick
Coventry, UK
T.Dinh@warwick.ac.uk

5th Andrew McGordon
WMG, University of Warwick
Coventry, UK
A.McGordon@warwick.ac.uk

6th Darren Hughes
WMG, University of Warwick
Coventry, UK
D.Hughes@warwick.ac.uk

***Abstract*— The majority of electrical failures in wind turbines occur in the semiconductor components (IGBTs) of converters. To increase reliability and decrease the maintenance costs associated with this component, several health-monitoring methods have been proposed in the literature. Many laboratory-based tests have been conducted to detect the failure mechanisms of the IGBT in their early stages through monitoring the variations of thermo-sensitive electrical parameters. The methods are generally proposed and validated with a single-phase converter with an air-cored inductive or resistive load. However, limited work has been carried out considering limitations associated with measurement and processing of these parameters in a three-phase converter. Furthermore, looking at just variations of the module junction temperature will most likely lead to unreliable health monitoring as different failure mechanisms have their own individual effects on temperature variations of some, or all, of the electrical parameters. A reliable health monitoring system is necessary to determine whether the temperature variations are due to the presence of a premature failure or from normal converter operation. To address this issue, a temperature measurement approach should be independent from the failure mechanisms. In this paper, temperature is estimated by monitoring an electrical parameter particularly affected by different failure types. Early bond wire lift-off is detected by another electrical parameter that is sensitive to the progress of the failure. Considering two separate electrical parameters, one for estimation of temperature (switching off time) and another to detect the premature bond wire lift-off (collector emitter on–state voltage) enhance the reliability of an IGBT could increase the accuracy of the temperature estimation as well as pre-mature failure detection.**

Keywords—IGBT, Bond wire lift-off, Renewable energy, Switching times, Wind turbine reliability, Temperature estimation

I. INTRODUCTION

Wind power is ranked as the number one power generation method amongst all renewable power sources, generating 14% of the EU's power demand of 362 TWh in 2018 [1]. Wind turbines (WTs) are mainly installed in remote, often offshore, areas which incurs additional expenditure associated with foundations, substations and subsea cables of offshore turbines as well as maintenance costs [2]. Reducing maintenance costs by enhancing the reliability of wind turbines can steadily reduce total expenditure. Failures within the electrical drivetrain, particularly in the power converters, are the major contributor to maintenance costs [3]. This restriction steadily increases the expenditure associated with foundations, substations and subsea cables of offshore WTs as well as their maintenance costs [4].

A health monitoring system of the electrical drivetrain can increase the probability of finding the early signs of degradation, preventing total failure by informing maintenance decisions. In this case, an effective maintenance schedule can be applied to avoid urgent maintenance and reduce the time taken to fix the problem [5].

Insulated gate bipolar transistors (IGBTs) are widely used in wind turbine power converters because of their availability and low costs. However, they also have the highest rate of failure amongst the components commonly found in WT converters. Thus, the reliability of the IGBTs plays a significant role in increasing availability of the WTs and minimizing the down time [6]. IGBTs are sensitive to temperature variations and electrical stresses. These stresses mainly originate from load swings, which accelerate their degradation. Because of wind speed variability (load swings), IGBT failures occur too frequently, prompting interest in improving their reliability in service.

A pitch controller can keep the generator speed constant for higher than rated wind speeds and hence temperature fluctuations for IGBT are almost constant for wind speed higher than rated. In fact, the generator speed remains constant for higher than rated wind speeds through pitch controller is applied. This can help to reduce load fluctuations and consequently temperature swings of the IGBTs in rotor side converter. However, not all WTs are equipped with a pitch angle controller. In addition, the

adverse effects of wind fluctuations are still of concern for lower-than-rated wind speeds even for WTs. The effect of using pitch angle controller on the operation of the IGBTs can be a further study.

Rapid cycling of load and temperature induces thermo-mechanical stresses in the IGBT. The multi-layer, multi-material structure (Fig 1) exhibits different thermal expansion coefficients for each layer that can result in increased thermally driven stresses [7].

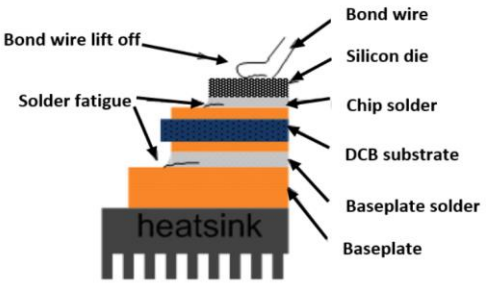

Fig 1. Multilayer structure of the IGBT [7]

Results from field tests show that two of the most common failures are bond wire lift-off (BWLO) [8] and solder fatigue (SF). To implement accurate health monitoring, tracking of temperature variation of the components is essential. However, the maximum temperature-induced stress is observed at the junction (silicon die) of the device, which cannot easily be directly measured [9]. In addition, it is difficult to track the transient changes of temperature due to the slow response of sensors. As an alternative to a physical sensor, several methods have been presented in the literature to estimate junction temperature, T_j, by monitoring certain electrical parameters.

These methods are either based on direct measurement or data-driven methods as summarized in Fig 2 [10-12]. The direct method is not widely used due to the high implementation costs and the requirement to access the inside of the module. Data-driven methods are most popular because of the accessibility of measurement points and these are mainly based on the monitoring thermo-sensitive electrical parameters of the IGBT.

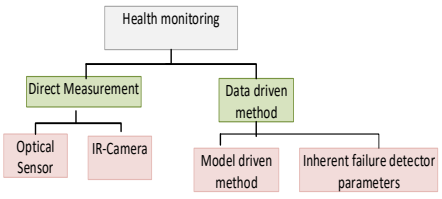

Fig 2. Health monitoring methods of an IGBT

In this paper, monitoring of switching off time (t_{off}) is proposed to estimate T_j as an electrical parameter independent of the progress of the BWLO failure. The detection of BWLO is achieved through a different electrical parameter, the collector emitter on-state voltage, $V_{CE,on}$. To test this approach, a calibration process has been carried out to understand the sensitivity of $V_{CE,on}$ to T_j at different IGBT health levels. A three-phase converter was designed and built to test the proposed estimation of T_j and detection of BWLO within an operational converter. While this paper has considered BWLO as the failure mode of interest, similar work has been done to detect another common failure mechanism, namely solder fatigue, within the operation of the converter.

II. Estimation of Temperature

A double pulse test was carried out to find the relationship between t_{off} and T_j for various load currents (Fig 3). Time t_{off} is a function of i_C and T_j [13]. The pulse durations for this test are short enough that self-heating is negligible. The case and heatsink temperatures are continuously monitored and logged using thermocouples to make sure there is no deviation from expected temperature. Here, t_{off} is defined as the sum of turn off delay time ($t_{d,off}$) and fall time (t_f), in (1), [14].

$$t_{off} = t_{d,off} + t_f \quad (1)$$

where $t_{d,off}$ is the time from when the gate-emitter voltage drops below 90% of the drive voltage to when the collector current drops below 90% of specified inductor current. Quantity t_f is the time taken for the collector current to drop from 90 to 10%.

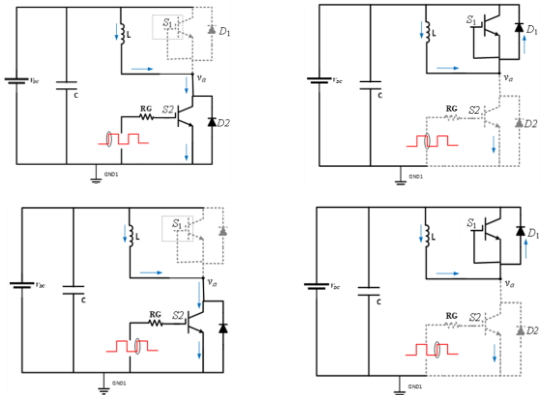

Fig 3. Electrical schematic of the double pulse test in four stages (top left: stage 1, top right: stage 2, bottom left: stage 3 and bottom right: stage 4)

Three different parameters: the gate-emiter voltage (V_{GE}); the collector-emitter voltage (V_{CE}); and collector current (i_c) are captured simultaneously to allow estimation of the switching times An example of a double-pulse result is shown in Fig 4.

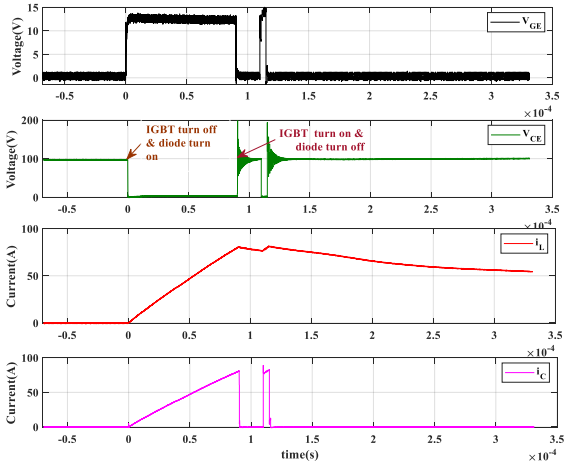

Fig 4. An example of the double pulse test output

Duration t_{off} is estimated at three different temperatures: 25ºC; 80 ºC; and 150ºC. Lines through three points and the corresponding linear equations are shown in Fig 5. The results show a positive correlation between t_{off} and T_j. The sensitivity of t_{off} to T_j is found to be higher than sensitivity of other switching time parameters, i.e t_{on}, $t_{d,on}$ and $t_{d,off}$ to T_j (as analysed in Table1). Based on the double-pulse test result, a linear model has been obtained (least squares fit) as a result of calibration, shown in Fig 6. Fig 6, seems to suggest three different loads (i_L), 40 A, 60 A and 80 A.

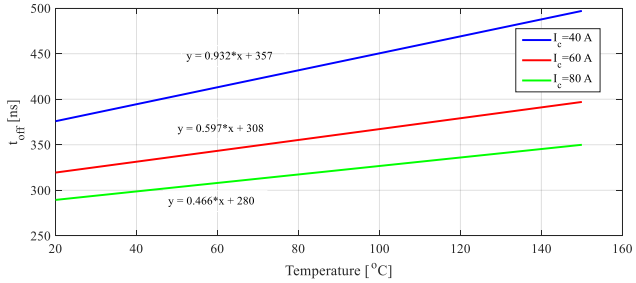

Fig 5. t_{off} versus T_j at different load currents

TABLE 1. Sensitivity of switching time to load current at constant DC-link voltage at 70 V

i_L	t_{on}	$t_{d,on}$	t_{off}	$t_{d,off}$
40 A	-0.028	-0.032	0.932	0.088
60 A	-0.036	-0.032	0.597	0.168
80 A	-0.044	-0.032	0.466	0.248

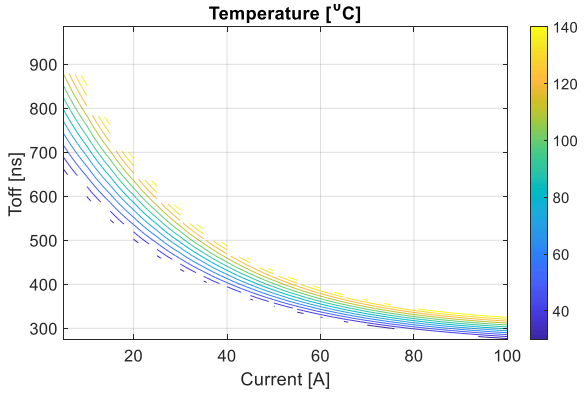

Fig 6. A 2D contour plot for t_{off} at 70 V

As previously mentioned, T_j increases in the presence of failure mechanisms and consequently changes in T_j can be a symptom of failure in an IGBT. Understanding the sensitivity of switching off time (t_{off}) to the progress of BWLO is therefore necessary. The lower the sensitivity to this failure, the more accurate the estimation of T_j. In this paper, BWLO is simulated by manual cutting of the bond wires, shown in Fig 7.

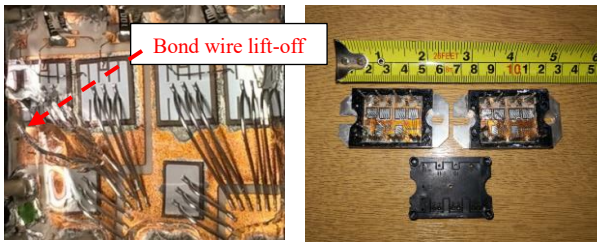

Fig 7. Imposing BWLO on the IGBT

Recall that t_{off} is the sum of t_f and $t_{d,off}$ (1). Fig 8 shows that t_f increases as the number of cut bond wires increases, whereas $t_{d,off}$ reduces significantly. The x-axis in Fig. 8 shows the number of cut bond wires from 0 (healthy) to 5 (as many as can be cut before total failure). A significant increase in t_f (from 96.85 to 101.8 ns) can be seen. Sensitivity of t_{off} to the number of cut wires is shown in Table 2.

Table 2. Sensitivity of t_{off} to progress of bond wire lift-off

Progress of failure	Sensitivity of t_{off} (ns)
One wire cut	0.02
Two wires cut	0.03
Three wires cut	0.06
Four wires cut	0.04
Five wires cut	0.08

This significant change chould be due to the faster discharge of the IGBT parasitic capacitances within the progress of failure and decrease in length of Miller Plateau. The decrease in $t_{d,off}$ almost matches the increase in t_f, so t_{off} remains almost constant as BWLO failures progress. The sensitivity of t_{off} to the number of cut wires is approximately 0.02 ns, so t_{off} is almost independent of BWLO. This independency helps to make t_{off} a good candidate as a temperature sensor. It is necessary to mention that the variations of $t_{d,off}$ and t_f cannot alter the switching speed of the devices. In fact, the $t_{d,off}$ plus t_f (i.e, t_{off}) remains almost constant after cycling. The results show that t_{off} is not significantly changed in the presence of BWLO, making it the best choice for estimating of T_j.

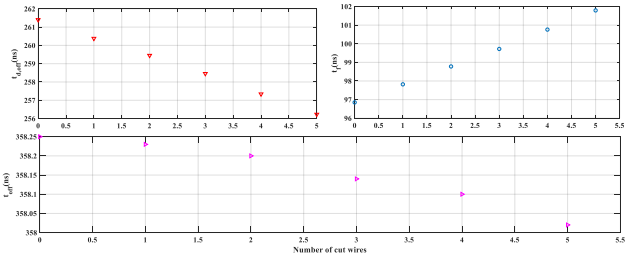

Fig 8. Sensitivity of $t_{d,off}$, t_f and t_{off} parameters to number of cut wires

III. Detection of Bond Wire Lift-Off

A. *Topology of interest*

Manufacturers have managed to increase current capacity and also improved heat tolerance of IGBTs by linking the chip and the emitter terminals with several parallel wires. These wires can become detached (lifted-off) during power cycling due to temperature stresses. From early failure when

one bond wire is lifted off to almost 65% of the wires lifted off, the IGBT is still able to function, albeit with a significantly increased risk of total failure [12]. Voltage drop across the bond wires increases as bond wires come adrift because of the increased load current passing through the remaining wires.

B. Calibration of $V_{CE,on}$

A relationship between $V_{CE,on}$ and i_C and temperature has been obtained using the calibration circuit shown in Fig 9.

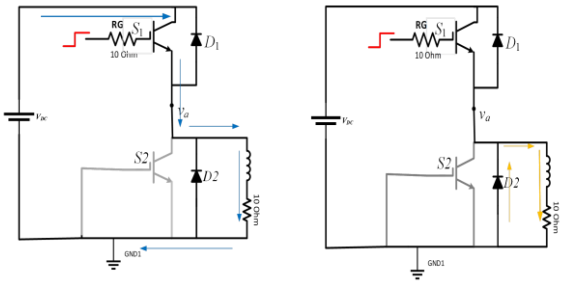

Fig 9. Calibration circuit used to evaluate variations of $V_{CE,on}$

There is a negative linear correlation between $V_{CE,on}$ and T_j as shown in Fig 10.

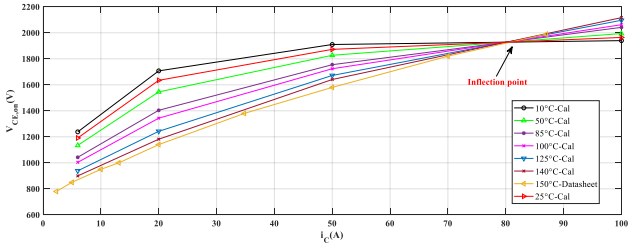

Fig 10. $V_{CE,on}$ vs i_c for various temperatures

The sensitivity of $V_{CE,on}$ to T_j reduces as i_c increases. Based on the calibration results, a linear relationship between $V_{CE,on}$, i_C and T_j can be found in (2-4). Here T_x represents the simulations T_j when $V_{CE,on_X}(Cal)$ desired to be measured.

$$V_{CE,on_{150C}} = -0.072i_C^2 + 21i_c + 75 \quad (2)$$

$$V_{CE,on_{25C}} = -(8.5e^{-5} \times i_C^4) + (0.02i_C^3) - (1.7i_C^2) + (66ic) + 860 \quad (3)$$

$$V_{CE,on_X}(Cal) = V_{CE,on_{25C}}\left(1 - \frac{T_x - T_{25}}{T_{150} - T_{25}}\right) + V_{CE,on_{150C}}\left(\frac{T_x - T_{25}}{T_{150} - T_{25}}\right) \quad (4)$$

The higher sensitivity of $V_{CE,on}$ to i_C rather than to T_j make this parameter a good failure detector for BWLO. Deviation of $V_{CE,on}$ for a given i_C and T_j can be used to indicate assess the possibility of BWLO. Fig 11 shows the detail.

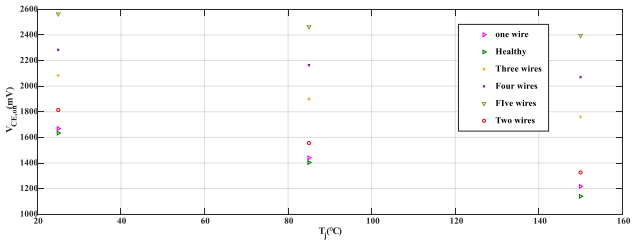

Fig 11. Sensitivity of $V_{CE,on}$ to BWLO coming from calibration board

IV. Detecting BWLO in a Three-Phase Converter

A. Test rig set up

A three-phase converter was constructed to examine the feasibility of measuring the proposed electrical parameters in an operational converter. The converter is connected to the three-phase permanent magnet machine of a micro WT, shown in Fig 12.

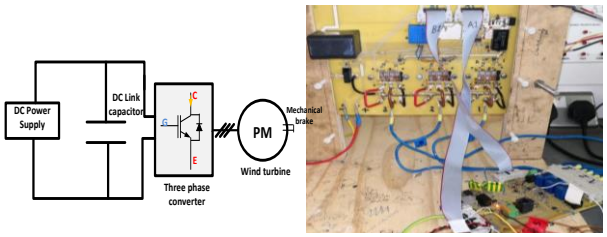

Fig 12. Test set up

Fig 13 shows the controller algorithm implementation in the microcontroller for both experiment and modelling (section V). The inner control loop is the current controller, based on the field-oriented control (FOC) [15]. A speed controller forms the outer loop. For the current controller, i_d^* is considered zero and torque is only controlled through i_q since flux is constant in a permanent magnet machine. A block diagram showing the controller parameters (kp and ki) of the current controller are shown in Fig 14 and obtained in (5-7). Figs 14 and 16 represent the control system shows in Fig 13 in further details. In Fig 14, i_{dq}^* represents reference current for both d-axis and q-axis (i.e, id_{ref} and iq_{ref} in Fig 13). ω_m^* and ω_m in Fig 16 refers to the speed-ref and speed in Fig 13.

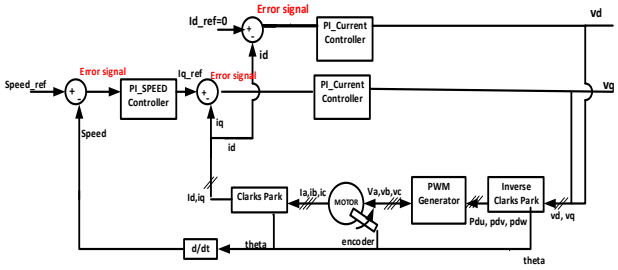

Fig 13. Controller(s) for the rotor side converter

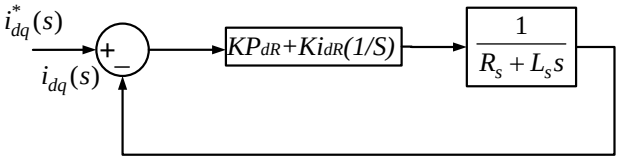

Fig 14. Current controller loop

$$\tau_R = \frac{1}{\sqrt{2}}, \quad \omega_{nR} = 2 \times \Pi \times f_{nR}, \quad f_{nR} = 2000 \quad (5)$$

$$Kp_{aR} = 2 \times L_s \times \tau_R \times \omega_{nR}\ , \ ki_{aR} = L_s \times ({\omega_{nR}}^2)) \quad (6)$$

$$kp_{dR} = kp_{aR} - (ki_{aR} \times \frac{T_s}{2}), \quad Ki_{dR} = Ki_{aR} \times T_s \quad (7)$$

To validate the current controller, $i_{q,ref}$ is set to 2 A. As shown in Fig 15, i_q follows $i_{q,ref}$.

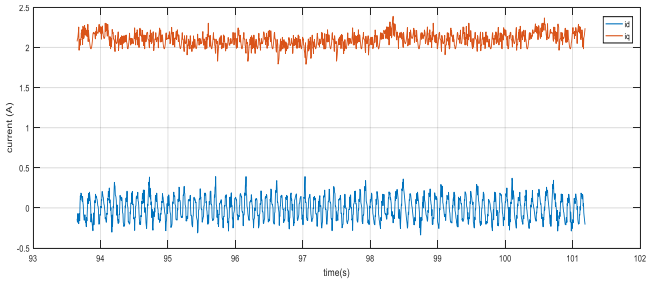

Fig 15. Validation of the current controllers

The block diagram for the speed controller is shown in Fig 16. Control parameters, KP_1 and KI_1 are calculated in (8) and (9).

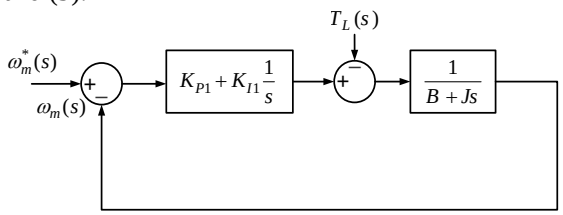

Fig 16. Speed controller block diagram

$$T = J\frac{d\omega_m}{dt} + \beta\omega_m\,, \qquad K_{P1} = 2 \times J \times \zeta_n \times \omega_n \quad (8)$$

$$K_{I1} = J \times {\omega_n}^2, \quad \omega_n = 2 \times \pi \times f_n \quad (\frac{rad}{s}) \qquad (9)$$

In Fig 17 the speed controller output (blue) approximately follows the speed reference input $speed_{ref}$ (red) as the reference speed varies from 0 to 180 rpm. The offset arises despite the integral action in the control loop because of numerical representation errors inside the controller.

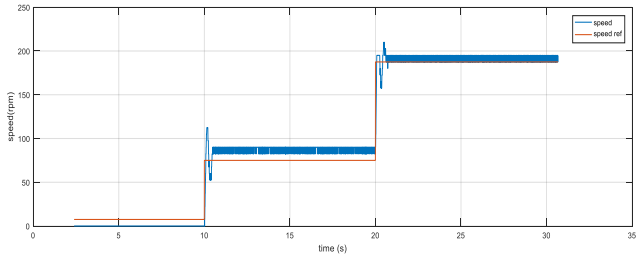

Fig 17. Validation of speed controller

B. Processing the measured data

Four parameters T_j , I_C , V_{CE} , V_{GE} were measured simultaneously. The output of the oscilloscope (2.5 GS/s) is saved for further processing. Parasitic oscillations are present in the V_{GE} and I_C signals, caused by inductance and capacitance within the IGBT and in the surrounding circuit. A state machine algorithm was developed to identify the first crossings of 10% and 90% values to obtain the switching times. These tests are run with three phase sinewave PWM mode at ambient temperature. This operating condition is more like that found in a real application compared to the conditions found in lab-based DC power cycling load tests with constant load current.

A histogram of all the data in each signal was been used to find out the high (100%) and low (0%) values at which the signal spends most of its time. From this, the 10% and 90% levels of V_{GE}, or other signals, can be found. Unfortunately, ringing can lead to several 10% and 90% candidate times being identified.

- $t_{d,on}$ - turn-on delay time is the time from when the gate emitter voltage rises past 10% of the drive voltage to when the collector current rises past 10% of the specified load current.
- $t_{d,off}$ - turn-off delay time is the time from when the gate emitter voltage drops below 90% of the drive voltage to when the collector current drops below 90% of specified load current. This gives an indication of the delay before current begins to transition in the load.
- t_r - rise time is the time between the collector current rising from 10% to 90% start to stop of the specified load current.
- t_f - fall time is the time between the collector current dropping from 90% to 10% start to stop of the specified load current.

To find 10% of i_C, the correct point is defined based on the closest points to 10% of V_{GE}. To find 90% of i_C during rise time, correct point is defined based on the closest point to 10% of i_C.This is shown more clearly in Fig 18.

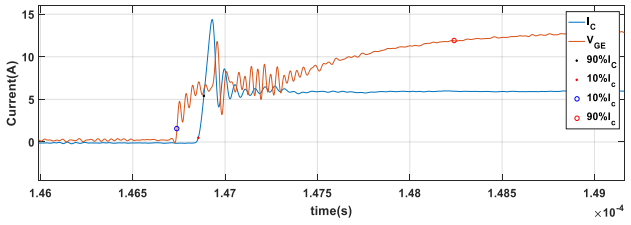

Fig 18: Switching on time of the IGBT

To find 90% of V_{GE} during the fall time, the correct point is defined based on considering the closest points to 10% of V_{GE} as a reference point. To find 10% of i_C, the correct point is defined based on the closest points to 90% of i_C as reference. This is shown more clearly in Fig 19.

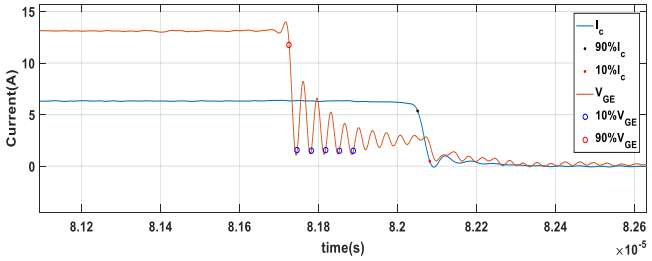

Fig 19: Switching off time of the IGBT

C. Health monitoring of IGBT in three phase converter

Quantity $V_{CE,on}$ is sensed using a precision difference amplifier that can accept a common mode voltage of up to 600 V. Variation of $V_{CE,on}$ has been studied in presence of BWLO for the three-phase converter (shown in Fig 11). The figure shows a pattern of $V_{CE,on}$ against current that represents the IGBT behavior for positive currents. As shown in Fig 20, $V_{CE,on}$ increases from healthy mode to 5 wires cut within operation of the converter.

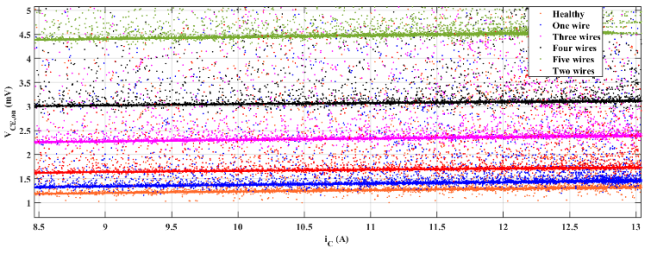

Fig 20. $V_{CE,on}$ versus i_c in different level of healthy status

Temperature T_j varies in time because of conduction power losses of the IGBT and hence the converter, and with the progress of the failure. T_j is estimated 65.2ºC by look up table shown in Figure 6.

V. Conclusion and Future Work

Unpredictable nature of wind speed causes stress, degradation and subsequent reduction in lifetime of IGBTs used in wind turbine converter. Healthy monitoring of the IGBT can diminish down time of the wind turbine converter. In this paper, two separates IGBTs' electrical parameters are used to estimate junction temperature (switching times-(2)) and to detect bond wire lift-off ($V_{CE,on}$). Collector emitter on-state voltage shows a positive sensitivity to the progress of the bond wire lift-off. With progress of bond wire lift-off, the voltage increase from its value in healthy status. The voltage has linear relation to collector current and junction temperature. Therefore, to use this voltage as a failure detector, the temperature and current should be simultaneously measured. Switching off time shows a negligible sensitivity to the progress of bond wire lift-off, which makes this parameter as a good choice of estimating junction temperature.

Acknowledgment

This research was conducted as a part of AEOLUS4FUTURE - Efficient harvesting of the wind energy" (H2020-MSCA-ITN-2014: Grant no. 643167), funded by the European Commission's Framework Program "Horizon 2020" (Marie Skłodowska-Curie Innovative Training Networks (ITN)). The work although largely carried out at the University of Birmingham benefitted from additional support from the University of Warwick.

References

[1] EREC, "Renewable energy technology roadmap by 2020", www.erec.org/fileadmin/erec_docs/Documents/Publications/Renewable_Energy_Technology_Roadmap.pdf [Accessed 23 March 2009].

[2] A. Keane, M. Milligan, C. J. Dent, "Capacity value of wind power", IEEE Trans power systems, Vol 26, 2011, pp. 564- 572.

[3] S. Georgilakis, "Technical challenges associated with the integration of wind power into power systems", Renewable and sustainable energy reviews, Vol 12, 2008, pp. 852-863.

[4] Shipurkar, "Improving the availability of wind turbine generator systems", PhD thesis, 2019.

[5] Wind Europe Report, 2017. https://windeurope.org/wp-content/uploads/files/about-wind/statistics/WindEurope-Annual-Statistics-2017.pdf

[6] S. Sheng, "Report on wind turbine subsystem reliability-a survey of various databases", NREL, 2013, https://www.nrel.gov/docs/fy13osti/59111.pdf.

[7] L. Ran, S. Konaklieva and P. McKeever, "Condition monitoring of power electronics", 2014.

[8] P. Tavner, B. Hahn, S. Faulstich, "Eliability & availability of wind turbine electrical & electronic components", 2011.

[9] N. Sathishkumar, Z. Ming, and Y. Ding, "A decision-making model for corrective maintenance of offshore wind turbines considering uncertainties", Energies, 2019.

[10] L. Kongjing, T. Gui Yun and L. Cheng, "State detection of bond wires lift-off in IGBT modules using eddy current pulsed thermography", IEEE Trans on power electronics, Vol 29, 2014, pp. 5000-5009.

[11] J. Bing, S. Xueguan, C. Wenping, "In Situ diagnostics and prognostics of solder fatigue in IGBT modules for electric vehicle drives", IEEE on power electronics, Vol 30, 2015.

[12] C. Zorn, N. Kaminski, "Temperature–humidity–bias testing on insulated-gate bipolartransistor modules-failure modes and acceleration due to high voltage," IET Power Electron, Vol 8, 2015.

[13] L. Hui, L. Shengquan, L. Yang, "Power cycling capabilities assessment of IGBT modules in wind power converter considering the wind turbulence effects," Int Conf on Power Electronics, 2014, pp. 30 -34.

[14] R. Moeini, P. Tricoli, H. Hemida, C. Baniotopoulos, "Increasing the reliability of wind turbines using condition monitoring of semiconductor devices: a review", IET Renewable Power Generation Journal, 2017.

[15] A. Daliento, P.Chouder, A. Guerriero, A. Massi, M. Pavan, R. Moeini, and P. Tricoli, "Monitoring, diagnosis, and power forecasting for photovoltaic fields: a review", Photoenergy, 2017, pp.13.